HHS Public Access

Author manuscript

Cancer Discov. Author manuscript; available in PMC 2020 August 01.

Published in final edited form as:

Cancer Discov. 2020 February ; 10(2): 198–213. doi:10.1158/2159-8290.CD-19-0966.

Efficacy and Determinants of Response to HER Kinase Inhibition in *HER2*-Mutant Metastatic Breast Cancer

Lillian M. Smyth[1,2], **Sarina A. Piha-Paul**[3], **Helen Won**[1], **Alison M. Schram**[1], **Cristina Saura**[4], **Sherene Loi**[5], **Janice Lu**[6], **Geoffrey I. Shapiro**[7], **Dejan Juric**[7], **Ingrid A. Mayer**[8], **Carlos L. Arteaga**[9], **Macarena I. de la Fuente**[10], **Adam M. Brufksy**[11], **Iben Spanggaard**[12], **Morten Mau-Sørensen**[12], **Monica Arnedos**[13], **Victor Moreno**[14], **Valentina Boni**[15], **Joohyuk Sohn**[16], **Lee S. Schwartzberg**[17], **Xavier Gonzàlez-Farré**[18], **Andrés Cervantes**[19], **François-Clement Bidard**[20], **Alexander N. Gorelick**[1], **Richard B. Lanman**[21], **Rebecca J. Nagy**[21], **Gary A. Ulaner**[1], **Sarat Chandarlapaty**[1], **Komal Jhaveri**[1], **Elena I. Gavrila**[1], **Catherine Zimel**[1], **S. Duygu Selcuklu**[1], **Myra Melcer**[1], **Aliaksandra Samoila**[1], **Yanyan Cai**[1], **Maurizio Scaltriti**[1], **Grace Mann**[22], **Feng Xu**[22], **Lisa D. Eli**[22], **Melanie Dujka**[22], **Alshad S. Lalani**[22], **Richard Bryce**[22], **José Baselga**[23], **Barry S. Taylor**[1], **David B. Solit**[1], **Funda Meric-Bernstam**[3], **David M. Hyman**[1]

[1]Memorial Sloan Kettering Cancer Center, New York, New York, USA. [2]St. Vincent's University Hospital, Dublin, Ireland. [3]MD Anderson Cancer Center, Houston, Texas, USA. [4]Vall d'Hebron University Hospital, Vall d'Hebrón Institute of Oncology (VHIO), Barcelona, Spain. [5]Peter MacCallum Cancer Centre, Melbourne, Victoria, Australia. [6]USC Norris Comprehensive Cancer Center, Los Angeles, California, USA. [7]Dana-Farber Cancer Institute, Boston, Massachusetts, USA. [8]Vanderbilt-Ingram Cancer Center, Nashville, Tennessee, USA. [9]UTSW Harold C. Simmons Comprehensive Cancer Center, Dallas, Texas, USA. [10]Sylvester Comprehensive Cancer Center, University of Miami, Miami, FL. [11]UPMC Hillman Cancer Center, Pittsburgh, Pennsylvania, USA. [12]Rigshospitalet University Hospital, Copenhagen, Denmark. [13]Gustave Roussy, Paris, France. [14]START Madrid Fundación Jimenez Diaz, Madrid, Spain. [15]START Madrid Hospital Universitario HM Sanchinarro, Madrid, Spain. [16]Yonsei Cancer Center, University College of Medicine, Seoul, Korea. [17]West Cancer Center, University of Tennessee, Memphis, Tennessee, USA. [18]Hospital Universitari Quirón Dexeus, Barcelona, Spain. [19]CIBERONC, Biomedical Research Institute

Corresponding Author: David M. Hyman, Memorial Sloan Kettering Cancer Center, 1275 York Avenue, New York Avenue, New York, NY 10065, USA. Phone: 646-888-4544; Fax: 646-888-4268; hymand@mskcc.org.

Author Contributions

L.M.S., S.P.-P., H.H.W., A.M.S., and D.M.H. contributed equally to this work.

A.N.G. analyzed genomic data.

A.S. collected, processed, and analyzed cfDNA.

G.A.U. developed the PET Response Criteria, analyzed all PET response data, and provided critical revision of manuscript.

C.Z., S.D.S., and M.M. helped collect and monitor patient samples and clinical and sequencing data.

Y.C. and M.S. modeled the HER2 mutations in vitro.

H.H.W. performed all computation analysis, interpreted data, and wrote the first draft of manuscript.

R.L. and B.N. performed cfDNA analyses

F.X., L.D.E., G.M., M.D., A.S.L., and R.B. were responsible for study development and supervision.

S.P.-P., A.M.S., C.S., S.L., J.L., G.I.S., D.J., I. M., C.L.A., M.I.dl.F., A.M.B., I.S., M.M-S., M.A., V.M., V.B., J.-H.S., L.S., S.V., X.G.-F., A.C., F.-C.B., S.C., K.J., E.I.G., and F.M.B enrolled patients and interpreted data.

A.M.S. enrolled patients, interpreted data, provided cfDNA analysis, and drafted the manuscript.

B.S.T. supervised the computational analyses.

D.M.H., L.M.S., and D.B.S. enrolled patients and analyzed and interpreted data.

J.B. enrolled patients, analyzed data, and wrote the first draft of manuscript.

D.M.H., J.B., L.M.S., H.H.W., and D.B.S. wrote the manuscript with input from all authors.

INCLIVA, University of Valencia, Spain. [20]Institut Curie, Paris, France. [21]Guardant Health, Redwood City, California, USA. [22]Puma Biotechnology, Inc., Los Angeles, California, USA. [23]Currently AstraZeneca, Cambridge, UK, previously Memorial Sloan Kettering Cancer Center, New York, New York, USA

Abstract

HER2 mutations define a subset of metastatic breast cancers with a unique mechanism of oncogenic addiction to HER2 signaling. We explored activity of the irreversible pan-HER kinase inhibitor neratinib, alone or with fulvestrant, in 81 patients with *HER2*-mutant metastatic breast cancer. Overall response rate was similar with or without estrogen receptor (ER) blockade. By comparison, progression-free survival and duration of response appeared longer in ER+ patients receiving combination therapy, although the study was not designed for direct comparison. Pre-existent concurrent activating *HER2* or *HER3* alterations were associated with poor treatment outcome. Similarly, acquisition of multiple *HER2*-activating events, as well as gatekeeper alterations, were observed at disease progression in a high proportion of patients deriving clinical benefit from neratinib. Collectively these data define *HER2* mutations as a therapeutic target in breast cancer and suggest that co-existence of additional *HER* signaling alterations may promote both *de novo* and acquired resistance to neratinib.

Keywords

metastatic breast cancer; HER2-mutant; neratinib; precision medicine; targeted therapy

Introduction

Somatic mutations in *HER2* (also known as *ERBB2*) occur in approximately 3% of breast cancers, predominantly in the hormone receptor-positive (HR+) HER2-negative (HER2–, non-amplified) subtype[1–4]. These mutations are further enriched in patients with lobular histology, where the rate may be as high as 10%[5,6]. A subset of *HER2* mutations are activating and associated with worse prognosis[3,7–9].

The therapeutic relevance of HER2-directed therapy in *HER2*-mutant breast cancers is an area of ongoing investigation[1,3,10,11]. We previously reported results from the multicenter, multi-histology phase 2 ‘basket’ trial of single-agent neratinib in *HER2*-mutant advanced solid tumors (SUMMIT;). In that analysis, the greatest antitumor activity was observed in patients with breast cancer, satisfying the primary efficacy endpoint in this tumor-specific cohort[10]. Although some patients with *HER2*-mutant breast cancer exhibited dramatic responses to neratinib, these responses were generally short-lived and the median progression-free survival (PFS) on neratinib was only 3.5 months.

In addition to its role in breast cancer initiation, HER2 signaling activation has been identified as a mechanism of endocrine therapy resistance[4,12–17]. Moreover, feedback between HER2 and estrogen receptor (ER) signaling has been postulated to be reciprocal, such that inhibition of either pathway may result in upregulation and activation of the

other[18,19]. Indeed, treatment with neratinib induces ER-dependent gene transcription in HER2-positive (HER2+) breast cancer cell lines[20,21] and has been demonstrated to overcome endocrine resistance in *HER2*-mutant breast cancer cell lines and xenografts[14,17]. Consistent with these observations, the greatest benefit of neratinib as extended adjuvant therapy in HER2+ breast cancer in the ExteNet trial was in the ER-positive (ER+) subgroup, most of whom were receiving concurrent endocrine therapy[22].

We therefore hypothesized that simultaneously targeting HER2 and ER might result in synergistic antitumor activity in patients with HR+, *HER2*-mutant breast cancer. To evaluate this prospectively, we amended SUMMIT to add a cohort testing the combination of neratinib and fulvestrant, a selective ER degrader. We utilized the SUMMIT clinical trial platform to explore the genomic determinants of response to neratinib-containing therapy, as well as mechanisms of primary and acquired resistance through molecular characterization of tissue and plasma samples.

Results

Patient Characteristics

In total, 81 patients with *HER2*-mutant metastatic breast cancer were enrolled (Supplementary Table S1), including 34 patients who received neratinib monotherapy (23 HR+, 11 HR negative [HR–]) and 47 who received neratinib plus fulvestrant (all HR+). To further facilitate demographic comparisons between subgroups, patients who received neratinib monotherapy were further subdivided by ER status (Table 1). Patients with HR+ disease were initially enrolled into the neratinib monotherapy cohort; these patients were subsequently exclusively enrolled into the neratinib plus fulvestrant combination cohort after its opening in March 2015. Thus, there was no randomization of HR+ patients between neratinib monotherapy and combination therapy cohorts. Patients with HR- disease were enrolled to neratinib monotherapy throughout the study period. In total, 33% of patients had lobular breast cancer compared with the estimated 10% incidence in metastatic breast cancer overall, consistent with the enrichment of *HER2* mutations in this histology[24].

The ER+ monotherapy and combination therapy cohorts were generally well balanced for baseline characteristics, although there were some exceptions with potential implications for any efficacy comparisons across groups (Table 1). Overall, ER+ patients were heavily pre-treated, with a median of 5.5 and 4 total prior therapies in the monotherapy and combination therapy cohorts, respectively. The ER+ cohorts were also well balanced for prior fulvestrant exposure. By comparison, monotherapy patients had received more lines of chemotherapy than combination therapy patients (median [range]: 3 [1–6] versus 1 [0–6] line, respectively). Similarly, prior exposure to cyclin-dependent kinase (CDK)4/6 inhibitors was higher in the combination therapy cohort (43% versus 12%; P=0.003), likely reflecting the different periods during which these patients were enrolled relative to regulatory approval of CDK4/6 inhibitors in this indication. Interestingly, the median duration of prior CDK4/6 inhibitor-containing therapy across both cohorts was only 5.0 months (range: 0.4–17.4 months).

In total, 22 unique *HER2* mutations were observed (Fig. 1A). There was no significant difference between the two cohorts for domains mutated, genomic alteration class, or individual variants. The majority were missense mutations (65/81, 80%), followed by exon 20 insertions (15/81, 19%) (Supplementary Table S2). At the individual variant level, the most common mutant alleles included L755 (19/81, 23%), V777 (14/81, 17%), S310 (10/81, 12%), D769 (8/81, 10%), G778_P780dup (8/81, 10%), and Y772_A775dup (7/81, 9%). To determine if this mutational pattern was consistent with the broader distribution of *HER2* mutations in both breast and other cancers, we performed a population-scale analysis to discover hotspot mutations in *ERBB2* in 42,434 retrospectively and prospectively sequenced samples from patients with cancer using an established computational framework[25]. Overall, 73% (16/22) of all unique *HER2* mutations observed occurred at statistically significant hotspots based on this analysis. At the patient level, 93% (75/81) of patients enrolled in SUMMIT harbored at least one *HER2* mutation at a known hotspot. Overall, based on this analysis and other genomic landscape studies, the *HER2* mutational pattern across the monotherapy and combination therapy cohorts was consistent with the expected distribution of *HER2* mutations in breast cancer.

Efficacy

In total, 82% (28/34) of monotherapy-treated and 83% (39/47) of combination-treated patients had Response Evaluation Criteria in Solid Tumors (RECIST)-measurable disease at baseline. Patients with RECIST non-measurable disease, most often confined to the bones, were primarily evaluated by ^{18}F-fluorodeoxyglucose-positron-emission tomography (FDG-PET) as previously described[26]. Key efficacy endpoints are shown in Fig. 1B and Table 2. Of note, the study was not designed for statistical analysis of the direct comparison of efficacy in the monotherapy and combination therapy cohorts. In monotherapy-treated patients, the confirmed overall response rate (ORR) was 17.4% (95% confidence interval [CI]: 5.0–38.8) in patients with ER+ disease and 36.4 (95% CI: 10.9–69.2) in those with ER– disease. In combination therapy-treated ER+ patients, the ORR was 29.8% (95% CI: 17.3–44.9%). In monotherapy-treated patients, the median progression-free survival (PFS) was 3.6 months (95% CI: 1.8–4.3) in ER+ disease and 2.0 months (95% CI: 1.0–5.5) in ER– disease; combination-treated patients had a median PFS of 5.4 months (95% CI: 3.7–9.2 months) (Supplementary Fig. S1A, 1B). Finally, the median duration of response (DOR) in monotherapy patients was 6.5 months (95% CI: 3.7–not estimable [NE]) in ER+ disease and 3.8 months (95% CI: 3.7–NE) in ER– disease; combination-treated patients had a median DOR of 9.2 months (95% CI: 5.5–16.6 months). Similar outcomes were observed in patients with RECIST-measurable disease at baseline (Table 2).

In an attempt to understand how prior therapy may have conditioned response to neratinib combination therapy, we next conducted a retrospective, non-pre-specified analysis of efficacy based on prior exposure to CDK4/6 inhibitor or fulvestrant-containing regimens (Supplementary Table S3). In this exploratory analysis, prior exposure to fulvestrant (n=25) did appear to be associated with inferior outcome in patients receiving combination therapy. By comparison, prior CDK4/6 inhibitor treatment (n=20) was not clearly associated with outcome, although we cannot rule out whether such an effect would be observed in a larger and more rigorously controlled dataset.

Safety

The safety profile of neratinib was consistent with prior studies and comparable across the monotherapy and combination cohorts (Table 3). Across both cohorts, the most common treatment-emergent adverse events (AEs) of any grade were diarrhea (82%), fatigue (35%), nausea (44%), vomiting (28%), and constipation (36%). The most common grade 3 AE was diarrhea (25%; Supplementary Table S4). No patient discontinued treatment as a result of diarrhea. Neratinib dose reductions occurred in 10% of patients overall. Only two patients (2%) permanently discontinued neratinib due to an AE (one patient in the monotherapy cohort discontinued because of grade 2 ascites and fatigue unrelated to neratinib; one patient in the combination cohort discontinued because of grade 3 failure to thrive unrelated to neratinib).

Genomic Determinants of Response

To facilitate standardized genomic assessment and downstream analysis of pre-treatment material, central sequencing (Memorial Sloan Kettering-Integrated Mutation Profiling of Actionable Cancer Targets [MSK-IMPACT]; see Methods[27]) was performed based on sample availability. Given the largely similar efficacy profiles of the two cohorts (total n=81), samples were pooled for this analysis. Overall, central sequencing data were available for 56 patients (69%; Supplementary Fig. S2).

HER2 Biomarker Analysis

The locally reported *HER2* mutation was not confirmed by central assessment in six patients (6 of 56 eligible patients; 11%), none of whom responded to treatment. In two of these patients, local *HER2* testing results were consistent with a subclonal *HER2* mutation, potentially explaining the discordance with central testing. To more broadly assess the hypothesis that patients enrolled on the basis of a subclonal *HER2* mutation are less likely to respond to neratinib, we evaluated the clonality of *HER2* mutations via central testing. At least one *HER2* mutation was clonal in 93% (41/44) of patients evaluable for clonality analysis (Fig. 2A). Notably, none of the three patients with exclusively subclonal *HER2* mutations responded to treatment.

Sequencing also identified multiple, concurrent, and potentially activating alterations in *HER2* in 16% (7/44) of patients (Fig. 2A), including two with a second *HER2* mutation, three with concurrent *HER2* amplification, and two with both an additional mutation and amplification. Of note, four of the five patients with genomically amplified *HER2* by next-generation sequencing had previously been locally assessed as HER2-, consistent with prior experience that cascade testing based initially on immunohistochemistry and then fluorescence *in situ* hybridization may fail to identify a small proportion of HER2+ patients[4]. Interestingly, 86% (6/7) of patients with multiple pre-treatment *HER2*-activating events did not achieve clinical benefit.

Given the prevalence of patients whose pre-treatment *HER2*-mutant tumor was characterized by multiple *HER2* alterations (co-mutations, gene amplification), we hypothesized that these may represent a molecularly distinct subset of tumors that appear to select for the acquisition of multiple activating signaling events. We therefore analyzed 29,373 prospectively

sequenced advanced cancers (see Methods) to identify the broader prevalence of this phenomenon. Interestingly, the greatest relative frequencies of tumors harboring more than one *HER2* mutation were observed in bladder and breast cancers, the two cancer types with the highest overall rates of *HER2* mutations (Fig. 2B). Although this clinical sequencing cohort consisted of patients with advanced and often heavily pre-treated disease, the molecular subset of *HER2*-mutant tumors appeared to be independent of prior therapy; we identified a similar pattern and frequency of *HER2* mutations in the primary untreated tumors of The Cancer Genome Atlas (data not shown). Overall, these findings indicate a subset of tumors selected for acquisition of multiple *HER2* mutations early in tumorigenesis. As most of the affected patients in the trial and the broader prospective sequencing cohort had their concurrent *HER2* mutations present in 100% of sequenced cancer cells, we investigated whether these were present in *cis* (on the same allele) or in *trans*. Integrating physical read support and, where evaluable, allele-specific absolute copy-number analysis (Fig. 2C), we determined the genomic configuration of concurrent *HER2* mutations and found that 88% of cases analyzable by this methodology were present in *cis* (Fig. 2D), further suggesting that these tumors positively select for additional *HER2*-activating events.

Concurrent Genomic Events

We next sought to determine how concurrent genomic alterations might be associated with outcome to neratinib-containing therapy in a subset of patients with sufficient broad profiling sequencing data (see Methods, n=47; Supplementary Fig. S2). After excluding patients with exclusively subclonal *HER2* mutations (n=4), concurrent mutations in *TP53* were associated with lack of clinical benefit (nominal P=0.006), whereas mutations in ERBB3 trended toward the same relationship (nominal P=0.111; Fig. 3A). In total, eight patients (17%) had concurrent *ERBB2* and *ERBB3* mutations, four of which (50%) were *ERBB3* E928G hotspot mutations (Supplementary Table S5). Concurrent *ERBB2* and *ERBB3* mutations were mutually exclusive with the presence of multiple *ERBB2*-activating events, suggesting that *ERBB3* mutations may be selected for in a subset of tumors with only one *ERBB2* mutation to further augment HER kinase signaling[28].

Given the unexpectedly high rate of concurrent *ERBB2* and *ERBB3* alterations, we sought to determine whether *ERBB2* mutations were significantly associated with other activating events in the mitogen-activated protein (MAP) kinase pathway using the aforementioned broader cohort of prospectively sequenced cancers (n=29,373). Consistent with observations from the SUMMIT breast cohort, *ERRB2* mutations were significantly and specifically associated with concurrent *ERBB3* mutations ($P=2.9\times10^{-9}$) but not with other alterations of effectors of the MAP kinase pathway alterations (Fig. 3B). Interestingly, co-occurrence of MAP kinase pathway-activating events was *ERBB2* allele-specific, associated with missense mutations in the extracellular ($P=3.36\times10^{-5}$) and kinase ($P=1.02\times10^{-5}$) domains but not kinase-domain insertions (P=1; Fig. 3C). Collectively, these data suggest that a subset of *HER2*-mutant breast cancers will select for additional activating events in either *HER2* or *HER3*, observed in 32% (15/47) of this cohort, and that these concurrently mutated tumors may be more resistant to pharmacologic inhibition with neratinib.

Expanding analysis of co-alterations to the pathway level did not identify additional patterns of genomic activation associated with outcome. Tumor mutational burden (TMB; mutations/megabase) was, however, significantly lower in patients deriving benefit from treatment versus those with no benefit (median 3.9 versus 5.4 somatic variants per sample; P=0.01), suggesting that either tumors with higher TMB may be more likely to acquire passenger *HER2* mutations or the greater genomic complexity associated with higher TMB may limit benefit from HER2 inhibition.

Mechanisms of Acquired Resistance

We then investigated whether exposure to neratinib-containing therapy selected for genomic changes that could potentially explain the emergence of therapeutic resistance. To this end, we compared the genomic profiles of tumor samples (6 tissue, 13 cell-free DNA [cfDNA], 3 both, Supplemental Fig.S2) obtained before starting neratinib treatment and after progression in a subset of patients deriving significant clinical benefit.

Nine patients, most of whom achieved clinical benefit (two complete response [CR], five partial response [PR], and two stable disease [SD]), had paired archival or pre-treatment and post-treatment tissue samples and successfully completed central sequencing. Although 62% of genomic alterations (67% mutations and 56% copy-number alterations) were shared between the pre- and post-treatment tumors, considerable inter-patient variability existed (Fig. 4A). Of the private mutations, most were present only in the post-treatment sample (36% versus 2% in the pre-treatment sample alone), consistent with increasing genomic complexity acquired with time and under the selective pressure of pharmacologic inhibition.

The pre-treatment *HER2* mutation that formed the basis of enrollment was retained in the post-treatment tissue of all nine patients. Secondary alterations in *HER2* (four in total) were observed in post-treatment tumors from three patients (one CR and two PRs). Specifically, one patient gained an *ERBB2* amplification that targeted the mutant allele, the second acquired both a secondary clonal *HER2* mutation and amplification, and the third acquired a non-hotspot mutation in *HER2* (L785F) (Supplementary Table S6). Prior work has shown that *HER* L785F mutation induces a steric class with the reversible HER kinase inhibitor lapatinib[29], and similarly mutations in the *EGFR* paralogue L777 confer resistance to other irreversible pan-HER kinase inhibitors (Fig. 4B)[30,31]. To evaluate the possibility that alterations beyond acquired *HER2* mutations may be responsible for development of resistance, all gained or lost alterations annotated as oncogenic or occurring at previously established hotspots (see Methods) were examined. Beyond the acquired *HER2* alterations, only five additional non-*ERBB2* alterations met criteria for potential significance (Supplemental Fig. S3). These additional variants, including copy-number alterations in *CDKN2A/B*, *MYC*, and *MDM4* (one each) and mutations in *PIK3R1* and *ALK* (one each), involve heterogeneous cellular mechanisms and do not demonstrate clear convergence on a single pathway.

To further evaluate the frequency at which additional *HER2* mutations were potentially selected for after exposure to neratinib plus fulvestrant, we analyzed paired cfDNA samples from 16 patients, most of whom achieved clinical benefit (one CR, nine PRs, two SDs), including 13 additional patients with insufficient paired tissue sequencing data. Consistent

with observations from tumor tissue profiling, acquisition of one or more *HER2* mutations was observed in tumor-derived cfDNA from 44% (7/16) of these patients. All three patients in whom pre-treatment and post-progression tumor and plasma samples existed showed an acquired *HER2* alteration detected using at least one assay (Supplementary Table S6). In one patient, both tissue and plasma sequencing identified a new *HER2* amplification at disease progression. Interestingly, in this same patient, tissue and plasma sequencing each identified one acquired *HER2* mutation, although the specific variants differed between assays (S310Y and I767M, respectively), consistent with multiple dual *HER2*-mutant clones arising in the same patient. In the second patient, four new *HER2* mutations emerged in the plasma sample alone, albeit at low variant frequencies (0.09–0.96%). To verify this finding, we repeated deep sequencing on an orthogonal assay that also utilizes unique molecular identifier barcodes of a second independent plasma sample from the same patient and timepoint, and confirmed all four mutations at similar allele frequencies, excluding the possibility these were technical artifacts detected at the level of assay sensitivity. In the third patient, we detected an acquired *HER2* amplification in both the tissue and plasma samples. In all cases, the acquired *HER2* mutations occurred at allele frequencies 10–100 times lower than the antecedent *HER2* mutation. Overall, 62% (8/13) of emergent *HER2* mutations detected in cfDNA occurred at previously described hotspots (Fig. 4C). Two of the non-hotspot mutations were apparent *HER2* gatekeeper mutations, including the L785F described above. No two mutations in the same sample occurred close enough together to evaluate whether they occurred in the same allele. Integrating analyses across both tissue and cfDNA, eight of 22 patients (36%) with samples analyzed by either methodology exhibited acquisition of at least one new *HER2* alteration; all but one of these patients derived clinical benefit from neratinib-containing therapy. Beyond acquisition of *HER2* alterations, no other broader pattern was observed.

Discussion

Utilizing SUMMIT, a multi-histology, genomically driven basket study, we sequentially evaluated the efficacy of neratinib, with or without fulvestrant, in patients with *HER2*-mutant metastatic breast cancer. The ORRs were similar with monotherapy and the combination. However, PFS and DOR appeared somewhat longer with the combination, both for all patients and when the analysis was restricted to ER+ patients alone.Despite this finding, it is important to note that this study was not designed to formally compare efficacy in the two cohorts. In fact, there are noteworthy differences in the populations enrolled into each cohort. Specifically, CDK4/6 inhibitors were approved during the study, resulting in significantly higher rates of prior exposure to these agents in the combination cohort. The absence of a fulvestrant-only contemporary control group also somewhat complicates interpretation of the combination data. Nevertheless, the efficacy of neratinib with fulvestrant in patients with heavily pre-treated ER+ *HER2*-mutant metastatic breast cancer is encouraging and warrants additional investigation.

While recognizing the important limitations of any retrospective genomic analysis conducted in a relatively small patient population, this study nonetheless provided a platform upon which to start interrogating broader genomic factors underlying the heterogeneous response to HER kinase inhibition in *HER2*-mutant metastatic breast cancer. Integrating

deep genomic annotation with treatment outcomes, a broad pattern of observations emerged. We observed that concurrent *HER2* and/or *HER3* alterations at baseline appeared to predict for poor treatment outcomes. Potentially consistent with these observations, analyses of large prospective clinical sequencing studies demonstrated that concurrent *HER2* mutations appear most common in tumors with the highest rates of *HER2* mutations (breast and bladder cancers) and that the majority of these mutations occur on the same allele. These clinical sequencing studies also demonstrate enrichment for concurrent *HER2* and *HER3* mutations but no other specific MAP kinase pathway-activating mutations. Importantly, in patients deriving clinical benefit from neratinib-containing therapy, acquisition of additional *HER2*-activating events was observed in a high proportion of patients upon disease progression on neratinib. It is important to note that these acquired alterations were observed at low allele frequencies in cfDNA, consistent with subclonal events. We also cannot rule out the possibility that a subset of these detected acquired alterations, in particular those not occurring at known hotspots or previously characterized, may be biologically neutral passenger events.

Collectively, however, these data suggest that at least a subset of *HER2*-mutant tumors appear to select for multiple *HER2* or *HER3* alterations, which may consequently result in both *de novo* and acquired resistance to HER kinase inhibitors (Fig. 4D). This observation is consistent with prior genetically engineered models of *HER2*-mutant cancer, demonstrating that expression of a single copy of many *HER2* missense hotspot mutations results in incomplete pathway activation and was associated with a weak transformed phenotype[32]. Consistent with our proposed model for neratinib sensitivity, prior work with RAF-targeted therapies in $BRAF^{V600}$-mutant melanoma demonstrated that a threshold of pathway inhibition of approximately ≥80% was required to observe clinical responses[33]. Our data lead us to speculate that HER2 inhibitors with different mechanisms of action (e.g. kinase inhibitors in combination with antibodies that inhibit HER kinase dimer formation) may be worth testing in this setting.

Our findings build upon, and provide additional context to, prior work aimed at understanding the biologic role of *HER2* mutations in breast cancer. A previous proof-of-concept study of neratinib monotherapy in *HER2*-mutant breast cancer identified emergence of multiple *HER2* mutations in cfDNA from one patient, including both a gatekeeper alteration (T798I) and a hotspot activating alteration (T862A)[1]. Consistent with this, another group separately reported identification of a gatekeeper *HER2* T789I mutation in a *HER2*-mutant patient treated with neratinib[34]. Another group recently reported a case series of patients with ER+ breast cancer who developed emergence of *HER2*-mutations after exposure to various anti-estrogen therapies[14]. In this series, endocrine resistance was successfully reversed in one patient with the addition of neratinib. In *HER2*-amplified cancers, acquisition of activating *HER2* mutations has also been reported by multiple groups as a potential resistance mechanism to HER2 therapy[35,36]. Interestingly, we have previously shown that at least a subset of these acquired *HER2* mutations in HER2-positive breast cancers retain sensitivity to neratinib, despite conferring resistance to HER2-directed monoclonal antibodies and reversible kinase inhibitors[11].

In conclusion, these trial data provide additional clinical evidence that *HER2*-mutant tumors represent a distinct genomic subtype of breast cancers with oncogenic addiction and consequent sensitivity to HER kinase inhibition. The efficacy of neratinib in combination with fulvestrant was promising in this heavily pre-treated patient population. Integrated genomic analysis suggests that concurrent genomic events in *HER2* and *HER3* at baseline and progression may confer resistance to HER2 kinase inhibition. This finding provides a potential rationale for the combination of multiple HER2 inhibitors in *HER2*-mutant breast cancer, a therapeutic strategy that has already proven highly effective in *HER2*-amplified breast cancer[37]. To address this strategy, the SUMMIT trial has recently been amended to explore dual HER2 targeting with the combination of neratinib plus trastuzumab (plus fulvestrant in HR+ disease) in patients with *HER2*-mutant breast cancer.

Methods

Eligibility Criteria

Eligible patients were men and women aged ≥18 years with histologically confirmed *HER2*-mutant advanced breast cancer, an Eastern Cooperative Oncology Group performance status of 0–2, with adequate hematopoietic, hepatic, kidney, and cardiac function (defined as a left ventricular ejection fraction ≥50%). Patients were eligible regardless of the number of prior lines of chemotherapy or endocrine therapy, including fulvestrant.

HR+ disease was required for enrollment in the neratinib plus fulvestrant combination therapy cohort, but not for the neratinib monotherapy cohort. HR+ disease was defined as ≥1% ER+ or progesterone receptor-positive cells, according to American Society of Clinical Oncology/College of American Pathologists guidelines[38]. *HER2* mutations were identified through testing as obtained at each participating site; tissue- and plasma-based assays were accepted. Central confirmation of the *HER2* mutation was not required before study enrollment and was performed retrospectively.

Key exclusion criteria included prior therapy with HER tyrosine kinase inhibitors (HER2 monoclonal antibodies were permitted), prior receipt of a cumulative epirubicin dose of >900 mg/m^2 or cumulative doxorubicin dose of >450 mg/m^2, and unstable brain metastases (treated and/or asymptomatic brain metastases were allowed). The redacted text of the protocol is provided in the Protocol Appendix.

Study Design and Treatment

The open-label, single-arm, multi-cohort, multi-tumor, phase 2, ‘basket’-type SUMMIT trial was conducted at 23 centers internationally, 15 of which enrolled at least one patient with breast cancer. Enrollment to the monotherapy and combination therapy cohorts began on July 8, 2013, and March 17, 2015, respectively. Following opening of the combination cohort, enrollment to the monotherapy cohort was permitted only for patients with HR– breast cancer. Patients in the monotherapy cohort received neratinib 240 mg orally daily on a continuous basis. Patients in the combination therapy cohort additionally received fulvestrant 500 mg intramuscularly on Days 1, 15, and 29, then once every 4 weeks thereafter. All patients received mandatory loperamide prophylaxis during cycle 1 (see

Protocol Appendix for details). Patients were treated until disease progression, unacceptable toxicity, or withdrawal of consent. The protocol was approved by the institutional review boards of all participating institutions, and written informed consent was obtained for all patients before performing study-related procedures.

Assessments

Tumor response was assessed locally every 8 weeks by computed tomography, magnetic resonance imaging, and/or FDG-PET. Patients with measurable disease according to RECIST (version 1.1) were assessed primarily according to these criteria. The remaining patients with non-measurable disease (i.e. patients with bone-only disease) were evaluated for response by FDG-PET according to PET Response Criteria (Supplementary Table S7) – a modified version of the PET Response Criteria in Solid Tumors (PERCIST; version 1.0)[39], as previously reported[40]. AEs were classified according to the Common Terminology Criteria for AEs (version 4.0)[41] from consent until day 28 after discontinuation of study treatment.

Statistical Analysis

The data cutoff for this report was October 19, 2018. Efficacy and safety analyses were performed on all patients who received at least one dose of neratinib. The primary endpoint was ORR at week 8 (ORR8), as assessed by investigators according to RECIST or PET Response Criteria (for those with RECIST non-measurable disease at baseline). Secondary endpoints included: confirmed ORR; best overall response (BOR); clinical benefit rate (CBR), defined as confirmed BOR of CR, PR, or SD for at least 24 weeks; duration of response (DOR); PFS; and safety.

For each cohort, a Simon optimal two-stage design with a true ORR8 ≤10% was considered unacceptable (null hypothesis), whereas a true ORR8 ≥30% (alternative hypothesis) merited further study. Efficacy in each cohort was analyzed independently and the study was not designed to formally compare efficacy across cohorts. DOR, PFS, and overall survival were estimated using the Kaplan–Meier method. The Clopper–Pearson method was used to calculate 95% CIs for ORR8, ORR, BOR, and CBR. Individual associations between genomic alterations and response were assessed by either Fisher's exact or chi-squared tests (where appropriate) and corrected for multiple hypothesis testing[42]. Such testing was performed to compare gene-level associations between the dichotomous clinical benefit groups. All statistical analyses were performed using SAS (version 9.4; SAS Institute Inc., Cary, NC, USA) and R software[43]. All figures were generated using R software.

Central Sequencing and Broad Profiling Genomic Analyses

Collection of archival tumor tissue samples and cfDNA from plasma was mandatory before treatment. cfDNA was also collected from plasma at each radiological response assessment and at progression. Before protocol version 3, patients were offered the option of having fresh biopsies taken pre-treatment and at progression. From protocol version 3 onwards, pre-treatment biopsy became mandatory. DNA from formalin-fixed paraffin-embedded archival tumor tissue samples (n=46) or cfDNA from plasma (n=10) and matched germline DNA (n=55) were sequenced using MSK-IMPACT to identify somatic single-nucleotide variants,

small insertions and deletions, copy-number alterations and structural variants[27]. Overall, an average 691-fold (range 209–1128 fold) coverage per tumor was achieved. These data were used to centrally confirm the reported *HER2* mutation and establish allele-specific DNA copy number, clonality, co-mutational patterns, TMB, and microsatellite instability status. Using MSK-IMPACT data, focal *HER2* amplifications were inferred using a fold-change cutoff of ≥1.5 (MSK-IMPACT tumor:normal sequencing coverage ratio) based on prior clinical validation[44]. Hotspot alterations were identified using a previously described method[25] and applied to an extended cohort of 42,434 sequenced human tumors. Additionally, alterations were annotated as oncogenic using OncoKB, a curated knowledge base of the oncogenic effects and treatment implications for mutations in a subset of cancer genes (http://www.oncokb.org[45]). For patients with centrally confirmed *ERBB2* mutations and matched germline DNA (n=44), total and allele-specific copy number, tumor purity, and ploidy were estimated using the Fraction and Allele-Specific Copy Number Estimates from Tumor Sequencing (FACETS) algorithm (version 0.5.6)[46]. FACETS data were used to infer clonality by calculating cancer cell fractions with 95% CIs as previously described[47,48]. In addition to *HER2* overexpression/amplification status, as routinely assessed at each site, *HER2* copy-number amplification was centrally evaluated by sequencing. In cases of concurrent *HER2* amplification, allele-specific copy number was inferred in a locus-specific and genome-wide manner using FACETS and integrated with mutant allele frequencies using previously published methods[47,48] to determine whether the mutant or wild-type allele was amplified. Additionally, for the subset of patients from the combination therapy cohort with sufficient remaining paired pre- and post-treatment cfDNA, key regions of 73 cancer-related genes were analyzed on a commercial targeted sequencing plasma assay (Guardant360; Guardant Health, Redwood City, CA, USA) using previously published methods[49] (Supplementary Fig. S2).

Pan-Cancer Mutational Data Analyses

Somatic tumor mutation data consisting of 29,373 pan-cancer tumor samples from 26,777 patients with advanced cancers sequenced with MSK-IMPACT were used in our analyses[27]. All samples were sequenced with one of three incrementally larger versions of the IMPACT assay, including 341, 410, and 468 cancer-associated genes. To identify somatic mutations in the MSK-IMPACT dataset with the greatest likelihood for being oncogenic drivers, we restricted out analyses to non-synonymous protein-coding variants, including missense, nonsense, and splice-site altering mutations, as well as small in-frame and frame-shift insertions and deletions (indels). These variants were annotated as known or likely oncogenic driver mutations using the OncoKB database[45]. We then retained any additional single-nucleotide polymorphisms and indels that arose at protein residues previously shown to be enriched for somatic mutations in tumors beyond a rate expected in the absence of selection[25]. Finally, all truncating mutations (including nonsense, splice-site, and frame-shift indels) in proteins annotated as known tumor suppressor genes based on OncoKB were also retained. All other mutations were excluded due to insignificant evidence for their role as oncogenic drivers.

Identification of Compound *ERBB2* Mutations

We identified all known and likely driver mutations arising in *ERBB2* from the MSK-IMPACT tumor mutation dataset. All samples harboring any putative *ERBB2* driver mutations were then inspected for possessing either 1 or 2+ distinct putative *ERBB2* driver mutations in the same tumor sample. The frequency of samples with 1 or 2+ *ERBB2* drivers in breast, bladder, or other cancer types was divided by the total number of non-hypermutated samples in each of the cancer types to obtain the percentages shown.

Phasing *ERBB2* Compound Mutations

All compound *ERBB2* mutations in the MSK-IMPACT dataset were subjected to *in silico* phasing to identify *ERBB2* mutations that could definitively be classified as arising in *cis* or *trans*. To this end, we used a combination of read-backed (i.e. physical) and inference-based approaches to phase the largest number of compound *ERBB2* mutations possible in the data. Briefly, for read-backed phasing, we inspected the raw sequencing BAM files in *ERBB2* compound-mutant samples for reads spanning the loci of both *ERBB2* variants. As individual sequencing reads will only align to single DNA fragments, we took the presence of three or more reads calling both *ERBB2* variants simultaneously to be sufficient evidence for the mutations arising in *cis* in the tumor genome. Conversely, when three or more reads called the mutant allele for one mutation and the wild-type allele for the other mutation, and *vice versa* (i.e. the mutations were called by mutually exclusive sets of at least three reads each), we took this to be evidence of a *trans* configuration, given knowledge that the two alleles were also both clonal in the tumor, as determined by FACETS allele-specific copy-number analysis[46]. Compound mutations not in either of these two scenarios were deemed ambiguous by read-backed phasing and attempted for phasing by inference.

ERBB2 Driver Co-incidence With *ERBB3* and Other MAP Kinase Drivers

We queried the complete MSK-IMPACT dataset of 25,197 non-hypermutated pan-cancer tumor samples for any known or likely oncogenic driver mutations. Samples with *ERBB2* driver mutations (n=436) were then queried for additional co-incident driver mutations in *ERBB3*, and in the absence of *ERBB3* drivers, queried for other MAP kinase pathway effector driver mutations. *ERBB2* driver-mutant samples were then categorized into three functionally distinct mechanisms of oncogenic *ERBB2* signaling: extracellular-domain hotspot mutations (hotspot mutations in *ERBB2* residues 23–652); kinase-domain hotspot mutations (hotspot mutations in *ERBB2* residues 720–987); and kinase-domain in-frame indels (small indels with *N*-terminal residues within the kinase domain). To test in-frame *ERBB2* indels, extracellular-domain hotspots, and kinase-domain hotspots for statistically significantly different rates of co-alteration with non-*ERBB2* MAP kinase driver mutations, we used a two-sided Fisher's test to compare the counts of non-*ERBB2* MAP kinase driver-mutant samples and non-*ERBB2* MAP kinase driver-less samples between pair-wise combinations of the three *ERBB2*-mutant categories.

Structural Impact of ERBB2 L785F on Neratinib Binding

The structure of ERBB2 bound to neratinib was obtained based on an experimentally derived structure of EGFR in complex with neratinib[50] to which the structure of the kinase

domain of ERBB2[51] was aligned. Briefly, the residues of EGFR undergoing hydrophobic interaction with the neratinib ligand were identified using UCSF Chimera[52], by searching for carbon atoms in hydrophobic residues of EGFR that were closer than 4Å to the carbon atoms of the neratinib molecule[53]. The structure of the kinase domain of ERBB2 was then aligned to these hydrophobic-interacting residues using Chimera's MatchMaker function. The structure of EGFR was then removed, leaving neratinib in place in the region of ERBB2 that aligned to its binding pocket in EGFR. Hydrophobic interactions between ERBB2 L785 and neratinib were subsequently determined by searching for carbon atoms in L785 within 4 Å of carbon atoms in the neratinib molecule.

Data Availability

All patient-level clinical outcome and genomic data are available on the cBioPortal.org (cbioportal.org/neratinibbreast).

Supplementary Material

Refer to Web version on PubMed Central for supplementary material.

Acknowledgments

We would like to thank patients and their families for participating in this study. Editorial support, not including writing, was provided by L. Miller and D. Carman (Miller Medical Communications Ltd.). This work was funded by Puma Biotechnology. M.S. is funded by NIH grant R01 CA190642, the Breast Cancer Research Foundation, Stand Up to Cancer (Cancer Drug Combination Convergence Team), the V Foundation, and the National Science Foundation.

Funding

The study was funded by Puma Biotechnology. Authors from Memorial Sloan Kettering were funded by NIH grant P30 CA008748.

M.S. is funded by the NIH grants P30 CA008748 and R01 CA190642, the Breast Cancer Research Foundation, Stand Up to Cancer (Cancer Drug Combination Convergence Team), the V Foundation and the National Science Foundation.

Disclosure of Potential Conflicts of Interest

L.M.S. has received research grants/funding (to her institution) from AstraZeneca, Puma Biotechnology Inc., and Roche Genentech. L.M.S has received payment for consultancy or advisory roles from AstraZeneca, Roche Genentech, Pfizer, and Novartis, honoraria from AstraZeneca, Roche Genentech, and Pfizer, and support covering travel, accommodations, and expenses from Pfizer, Puma Biotechnology Inc., and Roche Genentech.

S.P.-P. has received research grants/funding (to her institution) from AbbVie, Inc.; Aminex Therapeutics; BioMarin Pharmaceutical, Inc; Boehringer Ingelheim; Bristol-Myers Squib; Cerulean Pharma Inc.; Chugai Pharmaceutical Co., Ltd; Curis, Inc.; Five Prime Therapeutics; Flex Bio, Inc.; Genmab A/S; GlaxoSmithKline; Helix BioPharma Corp.; Incyte Corp.; Jacobio Pharmaceuticals Co., Ltd.; Medimmune, LLC.; Medivation, Inc.; Merck Sharp and Dohme Corp.; NewLink Genetics Corporation/Blue Link Pharmaceuticals; Novartis Pharmaceuticals; Pieris Pharmaceuticals, Inc.; Pfizer; Principia Biopharma, Inc.; Puma Biotechnology, Inc.; Seattle Genetics; Taiho Oncology; Tesaro, Inc.; TransThera Bio; XuanZhu Biopharma; S.P.-P. has no personal conflicts to disclose.

H.H.W. has no conflicts to declare.

A.M.S. has no conflicts to declare.

C.S. reports grants to her institution from Roche/Genentech, Macrogenics, Pfizer, Piqur Therapeutics, Puma Biotechnology, Synthon Biopharmaceuticals and Novartis; and personal fees (consultancy services or advisory

boards) from Puma Biotechnology, Pfizer, Roche, AstraZeneca, Sanofi, Celgene, Daiichi Sankyo, Eisai, Genomyc Health, Novartis, Pierre Fabre, and Synthon Biopharmaceuticals.

S.L. receives research funding to her institution from Novartis, Bristol-Myers Squibb, Merck, Roche Genentech, Puma Biotechnology, Pfizer, and Eli Lilly. S.L. has acted as consultant (not compensated) to Seattle Genetics, Pfizer, Novartis, BMS, Merck, AstraZeneca, and Roche Genentech. S.L. has acted as consultant (paid to her institution) to Aduro Biotech.

J.L. has received research grants (to her institution) from Pfizer, Novartis and Genentech and consultation fees (advisory roles) for Pfizer, Novartis, Puma, and Radius.

G.I.S. has received research funding from Eli Lilly, Merck KGaA/EMD Serono, Merck, and Sierra Oncology. He has served on advisory boards for Pfizer, Eli Lilly, G1 Therapeutics, Roche, Merck KGaA/EMD Serono, Sierra Oncology, Bicycle Therapeutics, Fusion Pharmaceuticals, Cybrexa Therapeutics, Astex, Almac, Ipsen, Bayer, Angiex, Daiichi Sankyo, and Seattle Genetics.

D.J. has received consultation fees from Novartis, Genentech, Eisai, Ipsen, EMD Serono; and research funding from Novartis, Genentech, Eisai, EMD Serono, Takeda, Celgene, and Placon Therapeutics.

I.M. has received payment for consultancy or advisory roles from Novartis, Genentech, Lilly, AstraZeneca, GSK, Immunomedics, Macrogenics and Seattle Genetics and research funding (to her institution) from Novartis, Genentech, and Pfizer.

C.L.A. has received research grants from Puma Biotechnology, Pfizer, Lilly, Bayer, Takeda, and Radius. He holds stock options in Provista and Y-TRAP, and serves in an advisory role to Novartis, AbbVie, Merck, Lilly, Symphogen, Daiichi Sankyo, Radius, Taiho Oncology, H3Biomedicine, OrigiMed, Puma Biotechnology, Immunomedics, and Sanofi. He is a member of the Scientific Advisory Board of the Komen Foundation.

M.I.dl.F. has no conflicts to declare.

A.M.B. is a consultant for Puma, Roche, Novartis, Pfizer, Lilly.

I.S. has received research funding from Puma Biotechnology; support covering travel, accommodation and expenses from Pfizer, Novartis, and BMS and has no honoraria, advisory roles, or stock ownerships.

M.M.-S. has no conflicts to declare.

M.A. has received honorarium from AstraZeneca, consultation fees from Seattle Genetics, research funding from Puma Biotechnology (to institution) and Daiichi Sankyo (to institution) and travel fees from Roche Genentech.

V.M. has no conflicts to declare.

V.B. is the principal investigator of the SUMMIT trial and has received institutional funding from Puma Biotechnology.

J.S. reports grants from MSD, Roche, Novartis, AstraZeneca, Lilly, Pfizer, Bayer, GSK, CONTESSA, and Daiichi Sankyo outside the submitted work.

L.S. has no conflicts to declare.

S.V. has no conflicts to declare.

X.G.-F. has no conflicts to declare.

A.C. has received funding from Genentech, Merck Serono, Roche, Beigene, Bayer, Servier, Lilly, Novartis, Takeda, Astellas, Fibrogen, Amcure, Sierra Oncology, AstraZeneca, Medimmune, BMS, and MSD.

F.-C.B. has no conflicts to declare.

A.N.G. has no conflicts to declare.

R.L. is an employee of and stock owner of Guardant Health, Inc., a member of the Board of Directors and stock owner in Biolase, Inc., and an advisory board member and stock owner in Forward Medical, Inc.

B.N. is an employee of and stock owner of Guardant Health, Inc.

G.A.U. has no conflicts to declare.

S.C. has received research support (to institution) from Genentech, Novartis, Eli Lilly, Daiichi Sankyo, and Sanofi, and ad hoc consulting fees (to S.C.) from Eli Lilly, Novartis, Sermonix, Revolution Medicines, Context Therapeutics, and BMS.

K.J. has received honoraria as a consultant or advisory board member from Novartis, Spectrum Pharmaceuticals, ADC Therapeutics, Pfizer, BMS, Jounce Therapeutics, Taiho Oncology, Synthon and Lily Pharmaceuticals; and has received research funding (to the institution) from Novartis, Clovis Oncology, Genentech, AstraZeneca, ADC Therapeutics, Novita Pharmaceuticals, Debio Pharmaceuticals, Pfizer, and Zymeworks.

E.I.G. has no conflicts to declare.

C.Z. has no conflicts to disclose.

S.D.S. has no conflicts to declare.

M.M. has no conflicts to disclose.

A.S. has no conflicts to disclose.

Y.C. has no conflicts to disclose.

M.S. is on the advisory boards of Bioscience Institute and Menarini Ricerche, has received research funds from Puma Biotechnology, Daiichi Sankyo, Targimmune, Immunomedics, and Menarini Ricerche, is a co-founder of Medendi Medical Travel and in the past 2 years received honoraria from Menarini Ricerche and ADC Pharma.

G.M. was formerly employed by Puma Biotechnology.

F.X. is an employee and shareholder of Puma Biotechnology.

L.D.E. is an employee and shareholder of Puma Biotechnology.

M.D. is an employee and shareholder of Puma Biotechnology.

A.S.L.: is an employee and shareholder of Puma Biotechnology.

R.B. is an employee and shareholder of Puma Biotechnology.

J.B. is an employee of AstraZeneca. He is on the Board of Directors of Foghorn and is a past board member of Varian Medical Systems, Bristol-Myers Squibb, Grail, Aura Biosciences, and Infinity Pharmaceuticals. He has performed consulting and/or advisory work for Grail, PMV Pharma, ApoGen, Juno, Lilly, Seragon, Novartis, and Northern Biologics. He has stock or other ownership interests in PMV Pharma, Grail, Juno, Varian, Foghorn, Aura, Infinity Pharmaceuticals, ApoGen, as well as Tango and Venthera, of which is a co-founder. He has previously received honoraria or travel expenses from Roche, Novartis, and Eli Lilly.

B.S.T. has no conflicts to declare.

D.B.S. has no conflicts to declare.

F.M.-B. has no conflicts to declare.

D.M.H. reports receipt of personal fees from Chugai Pharma, CytomX Therapeutics, Boehringer Ingelheim, Genentech/Roche and AstraZeneca, and research funding from Puma Biotechnology, AstraZeneca, Loxo Oncology, and Bayer AG.

References

1. Ma CX, Bose R, Gao F, Freedman RA, Telli ML, Kimmick G, et al. Neratinib efficacy and circulating tumor DNA detection of HER2 mutations in HER2 nonamplified metastatic breast cancer. Clin Cancer Res 2017;23:5687–95. [PubMed: 28679771]

2. Zehir A, Benayed R, Shah RH, Syed A, Middha S, Kim HR, et al. Mutational landscape of metastatic cancer revealed from prospective clinical sequencing of 10,000 patients. Nat Med 2017;23:703–13. Erratum in: 2017;23:1004. [PubMed: 28481359]

3. Connell CM, Doherty GJ. Activating HER2 mutations as emerging targets in multiple solid cancers. ESMO Open 2017;2:e000279. [PubMed: 29209536]

4. Razavi P, Chang MT, Xu G, Bandlamudi C, Ross DS, Vasan N, et al. The genomic landscape of endocrine-resistant advanced breast cancers. Cancer Cell 2018;34:427–38.e6. [PubMed: 30205045]

5. Desmedt C, Zoppoli G, Gundem G, Pruneri G, Larsimont D, Fornili M, et al. Genomic characterization of primary invasive lobular breast cancer. J Clin Oncol 2016;34:1872–81. [PubMed: 26926684]

6. Deniziaut G, Tille JC, Bidard F-C, Vacher S, Schnitzler A, Chemlali W, et al. ERBB2 mutations associated with solid variant of high-grade invasive lobular breast carcinomas. Oncotarget 2016;7:73337–46. [PubMed: 27602491]

7. Bose R, Kavuri SM, Searleman AC, Shen W, Shen D, Koboldt DC, et al. Activating HER2 mutations in HER2 gene amplification negative breast cancer. Cancer Discov 2013;3:224–37. [PubMed: 23220880]

8. Wang T, Xu Y, Sheng S, Yuan H, Ouyang T, Li J, et al. HER2 somatic mutations are associated with poor survival in HER2-negative breast cancers. Cancer Sci 2017;108:671–7. [PubMed: 28164408]

9. Hyman DM, Taylor BS, Baselga J. Implementing genome-driven oncology. Cell 2017;168:584–99. [PubMed: 28187282]

10. Hyman DM, Piha-Paul SA, Won H, Rodon J, Saura C, Shapiro GI, et al. HER kinase inhibition in patients with HER2- and HER3-mutant cancers. Nature 2018;554:189–94. Erratum in: Nature. 2019;566:E11–2. [PubMed: 29420467]

11. Cocco E, Javier Carmona F, Razavi P, Won HH, Cai Y, Rossi V, et al. Neratinib is effective in breast tumor bearing both amplification and mutation of ERBB2 (HER2). Sci Signal 2018;11:pii: eaat9773. [PubMed: 30301790]

12. Benz CC, Scott GK, Sarup JC, Johnson RM, Tripathy D, Coronado E, et al. Estrogen-dependent, tamoxifen-resistant tumorigenic growth of MCF-7 cells transfected with HER2/neu. Breast Cancer Res Treat 1992;24:85–95. [PubMed: 8095168]

13. Wright C, Nicholson S, Angus B, Sainsbury JR, Farndon J, Cairns J, et al. Relationship between c-erbB-2 protein product expression and response to endocrine therapy in advanced breast cancer. Br J Cancer 1992;65:118–21. [PubMed: 1346366]

14. Nayar U, Cohen O, Kapstad C, Cuoco MS, Waks AG, Wander SA, et al. Acquired HER2 mutations in ER+ metastatic breast cancer confer resistance to estrogen receptor-directed therapies. Nat Genet 2019;51:207–16. [PubMed: 30531871]

15. Shou J, Massarweh S, Osborne CK, Wakeling AE, Ali S, Weiss H, et al. Mechanisms of tamoxifen resistance: increased estrogen receptor-HER2/neu cross-talk in ER/HER2-positive breast cancer. J Natl Cancer Inst 2004;96:926–35. [PubMed: 15199112]

16. Morrison G, Fu X, Shea M, Nanda S, Giuliano M, Wang T, et al. Therapeutic potential of the dual EGFR/HER2 inhibitor AZD8931 in circumventing endocrine resistance. Breast Cancer Res Treat 2014;144:263–72. [PubMed: 24554387]

17. Croessmann S, Formisano L, Kinch LN, Gonzalez-Ericsson PI, Sudhan DR, Nagy RJ, et al. Combined blockade of activating ERBB2 mutations and ER results in synthetic lethality of ER+/HER2 mutant breast cancer. Clin Cancer Res 2019;25:277–89. [PubMed: 30314968]

18. Arpino G, Wiechmann L, Osborne CK, Schiff R. Crosstalk between the estrogen receptor and the HER tyrosine kinase receptor family: molecular mechanism and clinical implications for endocrine therapy resistance. Endocr Rev 2008;29:217–33. [PubMed: 18216219]

19. Sudhan DR, Schwarz LJ, Guerrero-Zotano A, Formisano L, Nixon MJ, Croessmann S, et al. Extended adjuvant therapy with neratinib plus fulvestrant blocks ER/HER2 crosstalk and maintains complete responses of ER^{+}/$HER2^{+}$ breast cancers: Implications to the ExteNET trial. Clin Cancer Res 2019;25:771–83. [PubMed: 30274983]

20. Ribas R, Pancholi S, Rani A, Schuster E, Guest SK, Nikitorowicz-Buniak J, et al.Targeting tumour re-wiring by triple blockade of mTORC1, epidermal growth factor, and oestrogen receptor

signalling pathways in endocrine-resistant breast cancer. Breast Cancer Res 2018;20:44. [PubMed: 29880014]

21. Scaltriti M, Carmona FJ, Toska E, Cocco E, Hyman D, Cutler R, et al. Neratinib induces estrogen receptor function and sensitizes HER2-mutant breast cancer to anti-endocrine therapy. Eur J Cancer 2016;69(Suppl. 1):S125 (abstract 378).
22. Martin M, Holmes FA, Ejlertsen B, Delaloge S, Moy B, Iwata H, et al. Neratinib after trastuzumab-based adjuvant therapy in HER2-positive breast cancer (ExteNET): 5-year analysis of a randomised, double-blind, placebo-controlled, phase 3 trial. Lancet Oncol 2017;18:1688–700. [PubMed: 29146401]
23. Wolff AC, Hammond ME, Hicks DG, Dowsett M, McShane LM, Allison KH, et al. Recommendations for human epidermal growth factor receptor 2 testing in breast cancer: American Society of Clinical Oncology/College of American Pathologists clinical practice guideline update. Arch Pathol Lab Med 2014;138:241–56. [PubMed: 24099077]
24. Dossus L, Benusiglio PR. Lobular breast cancer: incidence and genetic and non-genetic risk factors. Breast Cancer Res 2015;17:37. [PubMed: 25848941]
25. Chang MT, Bhattarai TS, Schram AM, Bielski CM, Donoghue MTA, Jonsson P, et al. Accelerating discovery of functional mutant alleles in cancer. Cancer Discov 2018;8:174–83. [PubMed: 29247016]
26. Ulaner GA, Saura C, Piha-Paul SA, Mayer IA, Quinn DI, Jhaveri K, et al. Impact of FDG PET imaging for expanding patient eligibility & measuring treatment response in a genome-driven basket trial of the pan-HER kinase inhibitor, neratinib. Clin Cancer Res 2019 9 23 [Epub ahead of print].
27. Cheng DT, Mitchell TN, Zehir A, Shah RH, Benayed R, Syed A, et al. Memorial Sloan Kettering-Integrated Mutation Profiling of Actionable Cancer Targets (MSK-IMPACT IMPACT): a hybridization capture-based next-generation sequencing clinical assay for solid tumor molecular oncology. J Mol Diagn 2015;17:251–64. [PubMed: 25801821]
28. Jaiswal BS, Kljavin NM, Stawiski EW, Chan E, Parikh C, Durinck S, et al. Oncogenic *ERBB3* mutations in human cancers. Cancer Cell 2013;23:603–17. [PubMed: 23680147]
29. Trowe T, Boukouvala S, Calkins K, Cutler RE Jr, Fong R, Funke R, et al. EXEL-7647 inhibits mutant forms of *ErbB2* associated with lapatinib resistance and neoplastic transformation. Clin Cancer Res 2008;14:2465–75. [PubMed: 18413839]
30. Kannan S, Venkatachalam G, Lim HH, Surana U, Verma C. Conformational landscape of the epidermal growth factor receptor kinase reveals a mutant specific allosteric pocket. Chem Sci 2018;9:5212–22. [PubMed: 29997876]
31. Avizienyte E, Ward RA, Garner AP. Comparison of the EGFR resistance mutation profiles generated by EGFR-targeted tyrosine kinase inhibitors and the impact of drug combinations. Biochem J 2008;415:197–206. [PubMed: 18588508]
32. Zabransky DJ, Yankaskas CL, Cochran RL, Wong HY, Croessmann S, Chu D, et al. *HER2* missense mutations have distinct effects on oncogenic signaling and migration. Proc Natl Acad Sci U S A 2015;112:E6205–14. [PubMed: 26508629]
33. Bollag G, Hirth P, Tsai J, Zhang J, Ibrahim PN, Cho H, et al. Clinical efficacy of a RAF inhibitor needs broad target blockade in *BRAF*-mutant melanoma. Nature 2010;467:596–9. [PubMed: 20823850]
34. Hanker AB, Brewer MR, Sheehan JH, Koch JP, Sliwoski GR, Nagy R, et al. An acquired $HER2_{T798I}$ gatekeeper mutation induces resistance to neratinib in a patient with *HER2* mutant-driven breast cancer. Cancer Discov 2017;7:575–85. [PubMed: 28274957]
35. Xu X, De Angelis C, Burke KA, Nardone A, Hu H, Qin L, et al. HER2 reactivation through acquisition of the *HER2* L755S mutation as a mechanism of acquired resistance to HER2-targeted therapy in $HER2^+$ breast cancer. Clin Cancer Res 2017;23:5123–34. [PubMed: 28487443]
36. Zuo WJ, Jiang YZ, Wang YJ, Xu XE, Hu X, Liu GY, et al. Dual characteristics of novel *HER2* kinase domain mutations in response to HER2-targeted therapies in human breast cancer. Clin Cancer Res 2016;22:4859–69. [PubMed: 27697991]

37. Swain SM, Baselga J, Kim SB, Ro J, Semiglazov V, Campone M, et al.; CLEOPATRA Study Group. Pertuzumab, trastuzumab, and docetaxel in HER2-positive metastatic breast cancer. N Engl J Med 2015;372:724–34. [PubMed: 25693012]
38. Hammond ME, Hayes DF, Dowsett M, Allred DC, Hagerty KL, Badve S, et al. American Society of Clinical Oncology/College of American Pathologists guideline recommendations for immunohistochemical testing of estrogen and progesterone receptors in breast cancer. J Clin Oncol 2010;28:2784–95. [PubMed: 20404251]
39. Wahl RL, Jacene H, Kasamon Y, Lodge MA. From RECIST to PERCIST: Evolving considerations for PET response criteria in solid tumors. J Nucl Med 2009;50(Suppl. 1):122S–50S. [PubMed: 19403881]
40. Diamond EL, Subbiah V, Lockhart AC, Blay JY, Puzanov I, Chau I, et al. Vemurafenib for *BRAF* V600-mutant Erdheim-Chester disease and Langerhans cell histiocytosis: Analysis of data from the histology-independent, Phase 2, open-label VE-BASKET study. JAMA Oncol 2018;4:384–8. [PubMed: 29188284]
41. US Department of Health and Human Services, National Institutes of Health, National Cancer Institute. Common Terminology Criteria for Adverse Events (CTCAE). Version 4; 2009 Available from: https://evs.nci.nih.gov/ftp1/CTCAE/CTCAE_4.03/Archive/CTCAE_4.0_2009-05-29_QuickReference_8.5×11.pdf
42. Benjamini Y, Hochberg Y. Controlling the false discovery rate: a practical and powerful approach to multiple testing. J R Stat Soc Series B Stat Methodol 1995;57:289–300.
43. R Core Team. R: A language and environment for statistical computing. R Foundation for Statistical Computing, Vienna, Austria; 2016 http://www.R-project.org/.
44. Ross DS, Zehir A, Cheng DT, Benayed R, Nafa K, Hechtman JF, et al. Next-generation assessment of human epidermal growth factor receptor 2 (ERBB2) amplification status: Clinical validation in the context of a hybrid capture-based, comprehensive solid tumor genomic profiling assay. J Mol Diagn 2017;19:244–54. [PubMed: 28027945]
45. Chakravarty D, Gao J, Phillips SM, Kundra R, Zhang H, Wang J, et al. OncoKB: A precision oncology knowledge base. JCO Precis Oncol 2017;2017. doi: 10.1200/PO.17.00011.
46. Shen R, Seshan VE. FACETS: allele-specific copy number and clonal heterogeneity analysis tool for high-throughput DNA sequencing. Nucleic Acids Res 2016;44:e131. [PubMed: 27270079]
47. McGranahan N, Favero F, de Bruin EC, Birkbak NJ, Szallasi Z, Swanton C. Clonal status of actionable driver events and the timing of mutational processes in cancer evolution. Sci Transl Med 2015;7:283ra54.
48. Bielski CM, Donoghue MTA, Gadiya M, Hanrahan AJ, Won HH, Chang MT, et al. Widespread selection for oncogenic mutant allele imbalance in cancer. Cancer Cell 2018;34:852–62.e4. [PubMed: 30393068]
49. Odegaard JI, Vincent JJ, Mortimer S, Vowles JV, Ulrich BC, Banks KC, et al. Validation of a plasma-based comprehensive cancer genotyping assay utilizing orthogonal tissue- and plasma-based methodologies. Clin Cancer Res 2018;24:3539–49. [PubMed: 29691297]
50. Sogabe S, Kawakita Y, Igaki S, Iwata H, Miki H, Cary DR, et al. Structure-based approach for the discovery of pyrrolo[3,2-d]pyrimidine-based *EGFR* T790M/L858R mutant inhibitors. ACS Med Chem Lett 2012;4:201–5. [PubMed: 24900643]
51. Aertgeerts K, Skene R, Yano J, Sang BC, Zou H, Snell G, et al. Structural analysis of the mechanism of inhibition and allosteric activation of the kinase domain of HER2 protein. J Biol Chem 2011;286:18756–65. [PubMed: 21454582]
52. Pettersen EF, Goddard TD, Huang CC, Couch GS, Greenblatt DM, Meng EC, et al. UCSF Chimera–a visualization system for exploratory research and analysis. J Comput Chem 2004;25:1605–12. [PubMed: 15264254]
53. Ferreira de Freitas R, Schapira M. A systematic analysis of atomic protein-ligand interactions in the PDB. Medchemcomm 2017;8:1970–1981. [PubMed: 29308120]

SIGNIFICANCE

HER2 mutations define a targetable breast cancer subset, although sensitivity to irreversible HER kinase inhibition appears to be modified by the presence of concurrent activating genomic events in the pathway. These findings have implications for potential future combinatorial approaches and broader therapeutic development for this genomically-defined subset of breast cancer.

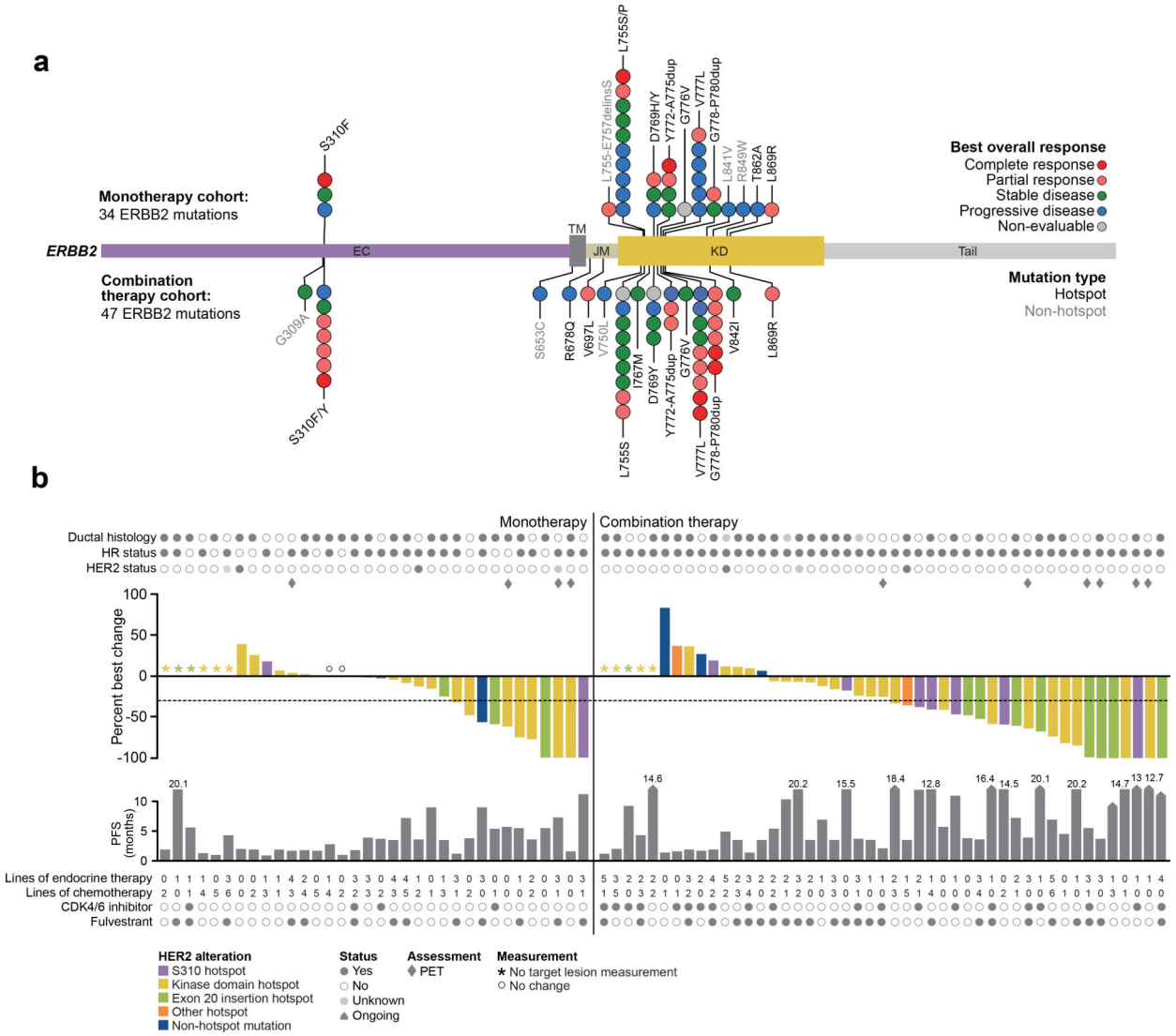

Figure 1. Response in the monotherapy and combination therapy cohorts.

(A) Distribution of *HER2* mutations observed in 34 monotherapy cohort patients (top) and 47 combination therapy cohort patients (bottom) positioned by their amino acid across the respective ERBB2 protein domains. Each unique mutation is represented by a circle and colored by their best overall response as indicated in the legend. (B) Treatment response and outcome for 34 monotherapy cohort patients (left) and 47 combination therapy cohort patients (right). Top graph represents percent best change of target lesion from baseline according to the appropriate response criteria (RECIST [version 1.1] or PET) with each bar colored by the respective *HER2* allele as indicated in the legend. Bottom graph represents PFS with arrows indicating patients with ongoing treatment. CDK, cyclin-dependent kinase; HR, hormone receptor; PET, positron-emission tomography; PFS, progression-free survival; RECIST, Response Evaluation Criteria in Solid Tumors.

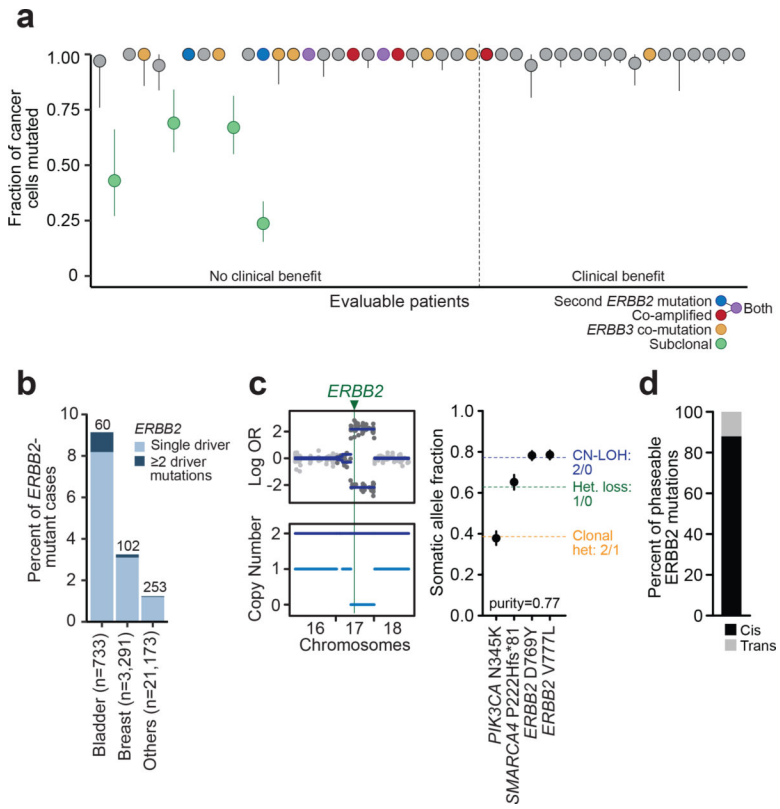

Figure 2. Clonality and co-mutation of *ERBB2*.

(A) Plot of the *ERBB2* clonality of 44 evaluable patients represented by cancer cell fractions with 95% confidence intervals and colored by additional *ERBB2/ERBB3* activating events as indicated by the legend. (B) Bar plot showing the overall percent of *ERBB2*-mutant cases and the number of cases with multiple *ERBB2* mutations (in dark blue) in the top mutated tumor types. (C) Allele-specific copy-number plot showing copy-neutral loss of heterozygosity (CN-LOH) at the *ERBB2* locus (left) and plot of the expected (dotted line) and observed allele frequencies with 95% binomial confidence intervals of the mutations to infer the phase (in *cis*) of the ERBB2 mutations (right). (D) Proportion of all phaseable *ERBB2* mutations across the broader prospective sequencing cohort occurring in *cis* versus in *trans*. Het, heterozygosity; OR, odds ratio.

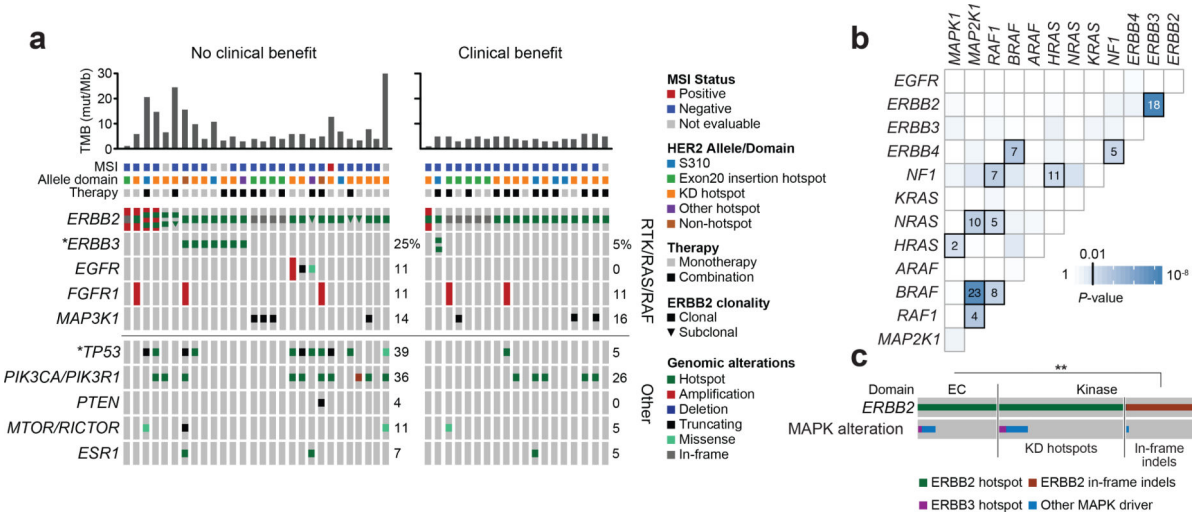

Figure 3. *ERBB2* and *ERBB3* co-mutation.

(A) OncoPrint of 47 evaluable patients grouped by clinical benefit (left, no clinical benefit, n=28; right, clinical benefit, n=19). Top bar chart represents the TMB shown in mutations per megabase (mut/Mb). MSI, allele domain and therapy type as indicated in the legend. Comprehensive oncoPrint showing alterations and clonality of *ERBB2* and other co-alterations in genes associated with RTK/RAS/RAF and other pathways. (B) Heatmap of co-alteration patterns in the MAPK pathway with significant associations highlighted and represented by the number of cases observed across the broader prospective sequencing cohort. (C) Condensed oncoPrint showing *ERBB2* missense and in-frame insertion or deletion (indel) mutations grouped by their respective protein domain and their co-occurrence patterns with *ERBB3* and other MAPK alterations. *Significant nominal Fisher's *P*-value; **Significant two-sided Fisher's *P*-value. EC, extracellular; KD, kinase domain; MAPK, mitogen-activated protein kinase; MSI, microsatellite instability; TMB, tumor mutational burden.

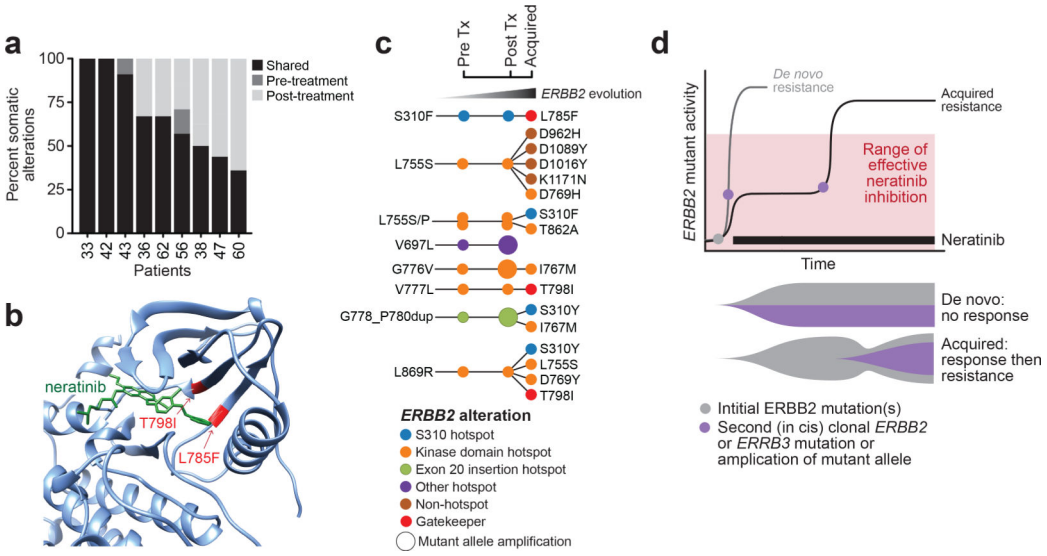

Figure 4. Mutant *ERBB2* evolution on therapy.

(A) Bar plot of nine patients with paired pre- and post-treatment tissue samples showing the proportion of alterations that were shared or exclusive. (B) Three-dimensional modeling structure showing two mutations (gatekeeper T798I, L785F) conferring steric hindrance to neratinib binding. (C) Overall *ERBB2* evolution in eight patients who acquired additional *ERBB2* alterations in either the tissue and/or cell-free DNA. Each circle represents an *ERBB2* mutation, colored by their respective allele/domain. (D) Conceptual schematic showing the impact of multiple activating events in *ERBB2/ERBB3* and potential mechanisms of *de novo* and acquired resistance to pharmacologic inhibition to neratinib over time. Tx, treatment.

Table 1.

Baseline demographic and disease characteristics

Characteristic	Neratinib monotherapy (*n*=34)		Neratinib + fulvestrant (*n*=47)
	ER+ (*n*=23)	ER− (*n*=11)	
Median age, years (range)	57 (37–78)	59 (52–80)	60 (43–87)
Female, *n* (%)	22 (95.7)	10 (90.9)	47 (100)
ECOG performance status, *n* (%)			
0	6 (26.1)	4 (36.4)	24 (51.1)
1	16 (69.6)	7 (63.6)	22 (46.8)
2	1 (4.3)	0	1 (2.1)
Post-menopausal, *n* (%)	21 (91.3)	10 (90.9)	42 (89.4)
Tumor histology, *n* (%)			
Ductal	15 (65.2)	9 (81.8)	27 (57.4)
Lobular	7 (30.4)	2 (18.2)	16 (34.0)
Other	1 (4.3)	0	4 (8.5)
***HER2* status[b] non-amplified, equivocal**	20 (87.0)	10 (90.9)	44 (93.6)
Visceral disease at enrollment, *n* (%)	18 (78.3)	7 (63.6)	37 (78.7)
Prior endocrine therapy[C], *n* (%)			
Aromatase inhibitor	14 (60.9)	1 (9.1)	31 (66.0)
Tamoxifen	8 (34.8)	0	9 (19.1)
Fulvestrant	12 (52.2)	1 (9.1)	23 (48.9)
Prior therapies[C], median (range)			
Total	5.5 (1–9)	2 (1–5)	4 (1–11)
Chemotherapy	3 (1–6)	2 (1–5)	1 (0–6)
Endocrine therapy	3 (1–5)	1 (1–1)	2 (0–5)
Prior targeted therapy, *n* (%)			
CDK4/6	2 (8.7)	2 (18.2)	20 (42.6)
PI3K/AKT/mTOR	7 (30.4)	1 (9.1)	10 (21.3)
***HER2* mutations**			
Kinase-domain hotspot	15 (65.2)	7 (63.6)	26 (55.3)
Exon 20 insertion hotspot	3 (13.0)	3 (27.3)	9 (19.1)
S310	3 (13.0)	0	7 (14.9)
Other	2 (8.7)	1 (9.1)	5 (10.6)

CDK, cyclin-dependent kinase; ECOG, Eastern Cooperative Oncology Group; ER+, estrogen receptor positive; ER−, estrogen receptor negative; mTOR, mammalian target of rapamycin; PI3K, phosphatidylinositol 3-kinase.

[a] Includes both primary and metastatic biopsies.

[b] As reported by local sites according to American Society of Clinical Oncology/College of American Pathologists or European Society for Medical Oncology guidelines[23].

[C] Any prior therapy in advanced or metastatic setting.

Table 2.

Treatment efficacy

	Neratinib monotherapy		
Response	**ER+**	**ER−**	**Neratinib + fulvestrant**
All patients (intent to treat)[a]	(*n*=23)	(*n*=11)	(*n*=47)
Confirmed overall objective response[b]**, *n* (%)**	4 (17.4)	4 (36.4)	14 (29.8)
Complete response	2 (8.7)	1 (9.1)	4 (8.5)
Partial response	2 (8.7)	3 (27.3)	10 (21.3)
Overall objective response rate (95% CI)	17.4 (5.0–38.8)	36.4 (10.9–69.2)	29.8 (17.3–44.9)
Clinical benefit rate[c]**, % (95% CI)**	30.4 (13.2–52.9)	36.4 (10.9–69.2)	46.8 (32.1–61.9)
Time to event (months), median (95% CI)			
Progression-free survival	3.6 (1.8–4.3)	2.0 (1.0–5.5)	5.4 (3.7–9.2)
Duration of response	6.5 (3.7–NA)	3.8 (3.7–NA)	9.2 (5.5–16.6)
RECIST-measurable disease only	(*n*=18)	(*n*=10)	(*n*=39)
Confirmed overall objective response[b]**, *n* (%)**	3 (16.7)	2 (20.0)	12 (30.8)
Complete response	1 (5.6)	1 (10.0)	2 (5.1)
Partial response	2 (11.1)	1 (10.0)	10 (25.6)
Overall objective response rate, % (95% CI)	16.7 (3.6–41.4)	20.0 (2.5–55.6)	30.8 (17.0–47.6)
Clinical benefit rate[c]**, % (95% CI)**	27.8 (9.7–53.5)	20.0 (2.5–55.6)	46.2 (30.1–62.8)
Time to event (months), median (95% CI)			
Progression-free survival	3.6 (1.8–4.3)	1.9 (1.0–5.4)	5.4 (3.5–10.3)
Duration of response	7.4 (3.7–NA)	3.8 (3.7–3.9)	9.0 (4.5–16.6)

CI, confidence interval; ER+, estrogen receptor positive; ER−, estrogen receptor negative; NA, not available; RECIST, Response Evaluation Criteria in Solid Tumors.

[a]Response is based on investigator-assessment per RECIST (version 1.1), in patients with measurable disease, or positron-emission tomography response criteria in patients without measurable disease.

[b]Confirmed no less than 4-weeks after the criteria for response are initially met.

[c]Clinical benefit is defined as confirmed best overall response of complete response, partial response of any duration or stable disease lasting for at least 24 weeks.

Table 3.

Adverse events[a]

Event	Neratinib monotherapy (*n*=34)		Neratinib + fulvestrant (*n*=47)	
	Any grade	Grade ≥3	Any grade	Grade ≥3
Any adverse event	33 (97.1)	16 (47.1)	47 (100)	23 (48.9)
Diarrhea	26 (76.5)	9 (26.5)	40 (85.1)	11 (23.4)
Fatigue	16 (47.1)	0	12 (25.5)	0
Nausea	15 (44.1)	0	21 (44.7)	0
Constipation	14 (41.2)	0	15 (31.9)	0
Vomiting	13 (38.2)	1 (2.9)	10 (21.3)	1 (2.1)
Abdominal pain	8 (23.5)	1 (2.9)	8 (17.0)	0
Decreased appetite	8 (23.5)	0	13 (27.7)	0
AST increased	7 (20.6)	3 (8.8)	3 (6.4)	1 (2.1)
Arthralgia	6 (17.6)	0	6 (12.8)	0
Pyrexia	6 (17.6)	0	4 (8.5)	0
Anemia	5 (14.7)	2 (5.9)	6 (12.8)	1 (2.1)
Dyspnea	5 (14.7)	2 (5.9)	6 (12.8)	1 (2.1)
Headache	5 (14.7)	0	6 (12.8)	0
ALT increased	4 (11.8)	1 (2.9)	2 (4.3)	0
Dehydration	4 (11.8)	2 (5.9)	2 (4.3)	0
Pruritus	4 (11.8)	0	4 (8.5)	0
Rash	4 (11.8)	0	7 (14.9)	0
Abdominal distension	4 (11.8)	0	2 (4.3)	0
Dry skin	3 (8.8)	0	9 (19.1)	0
Back pain	3 (8.8)	1 (2.9)	8 (17.0)	0
Insomnia	2 (5.9)	0	5 (10.6)	0
Peripheral edema	1 (2.9)	0	7 (14.9)	0
Weight decreased	1 (2.9)	0	5 (10.6)	0
Hot flash	0	0	5 (10.6)	0

[a]Regardless of attribution, occurring in ≥10% of patients.

ALT, alanine aminotransferase; AST, aspartate aminotransferase.